TRANSPORT PROBLEMS 2024 Volume 19 Issue 1
PROBLEMY TRANSPORTU DOI: 10.20858/tp.2024.19.1.09

Keywords: flow control; drag reduction; dimples; blowing; CFD; PIV; high-speed vehicles

Yevhenii SHKVAR[1], Jonas KANDUME[2*], Dmytro REDCHYTS[3]

THE KEY ROLE OF MODERN AERODYNAMIC TRENDS IN INCREASING THE ENERGY EFFICIENCY OF HIGH-SPEED VEHICLES

Summary. Based on the analysis of typical operating modes of modern high-speed trains and transport aircraft, the influence of various schemes of surface relief modification and blowing through it on aerodynamic drag has been thoroughly investigated. A set of several schemes of the combined effect of these two factors is proposed to create an easy-to-use, cheap-to-produce streamlined surface of the desired structure with a reliable and controllable effect of active influence on aerodynamic drag reduction. The potential effect of reducing aerodynamic drag has been verified by numerical and Particle Image Velocimetry experimental modeling. The proposed technological innovations are encouraging and relevant; by reducing energy costs, they increase the commercial and environmental attractiveness of their implementation.

1. INTRODUCTION

The well-known priorities in the development of transport are a steady increase in speed and a decrease in energy costs. In this regard, throughout the history of the development of high-speed transport, efforts have been made to optimize the shape of the vehicle body for the expected operating conditions. One of the important factors is the interaction of the vehicle with the air. Since the aerodynamic forces are proportional to the square (more precisely, taking into account the variability of the aerodynamic coefficient to the power of 1.8) of the speed, the role of perfect aerodynamics is constantly and rapidly increasing. Today, the shape of both transport airplanes and high-speed trains is in many ways similar and close to optimal. Thus, the shape (profile) drag component is already maximally minimized. As it follows from well-known estimates, under cruise modes of modern vehicles, the contribution of skin friction component in the total aerodynamic drag exceeds half for transonic transport aircraft (V=800-900 km/h, H=10-11 km) [1] and a third for high-speed trains (V=300-450 km/h, H=0 km) [2].

Therefore, new ideas and tools are needed to further improve the flow and reduce losses associated with aerodynamic drag. Moreover, as clearly follows from the above analysis, the main efforts should be concentrated precisely on skin friction drag reduction. One of the promising directions is to change the structure of the streamlined surface, which is directly related to hydrobionics. There are many vivid justifications in wildlife, where both the wings of birds and the skin of various hydrobionts are usually not smooth, having a regular microrelief. One of the best examples of the natural implementation of a highly developed micro-structured surface is the skin of sharks, which is covered with an array of microelements called denticles. These denticles are flexibly and independently of each other attached to the skin and regularly profiled with several (usually three to five) microgrooves.

[1] Zhejiang Normal University, College of Engineering; 688 Yingbin Road, Jinhua, Zhejiang Province, 321004, China; e-mail: eush@ukr.net; orcid.org/0000-0001-9589-5860
[2] Zhejiang Normal University, College of Engineering, 688 Yingbin Road, Jinhua, Zhejiang Province, 321004, China; e-mail: jonaskandume449@gmail.com; orcid.org/0009-0001-5614-8034
[3] Institute of Transport Systems and Technologies of the National Academy of Sciences of Ukraine; Pisarzhevsky 5, 49005 Dnipro, Ukraine; e-mail: redchits_da@ua.fm; orcid.org/0000-0001-8538-6026
* Corresponding author. E-mail: jonaskandume449@gmail.com

The purposes of this paper are to discuss promising areas of research on the modification of streamlined surface relief and to show an example of a rational combination of two related technologies: microblowing and dimples.

2. STREAMLINED SURFACE IMPROVEMENTS

Both in nature and in engineering, near-wall flow around any surface under practically realizable regimes is associated with the intensive formation of turbulence on the overwhelming area of the wetted surface in a narrow area called the boundary layer, where viscosity effects are most significantly manifested. Accordingly, here, turbulence acts physically as an additional physical effect and, according to its contribution, the prevailing dissipative factor. Therefore, it makes the main contribution to the formation of shear stresses, which lead to an increase in aerodynamic drag. That is why the main efforts in the development of drag reduction technologies are aimed at controlling the formation of turbulence. Since turbulence as a physical property inherent in a moving fluid cannot be eliminated globally for the entire streamlined surface, its local suppression or purposeful redistribution between its components of perturbed motion are the most relevant approaches. Since turbulence has a vortex structure and is characterized by a wide range of vortex scales [3] from very small – dissipative vorticity to large (about the boundary layer thickness) – inertial vortices that transfer turbulence along the flow (Fig. 1), the methodology of reducing aerodynamic friction drag is actually the control of vortices of various scales. A more detailed analysis of the most promising drag reduction methods based on this vortex concept is presented below.

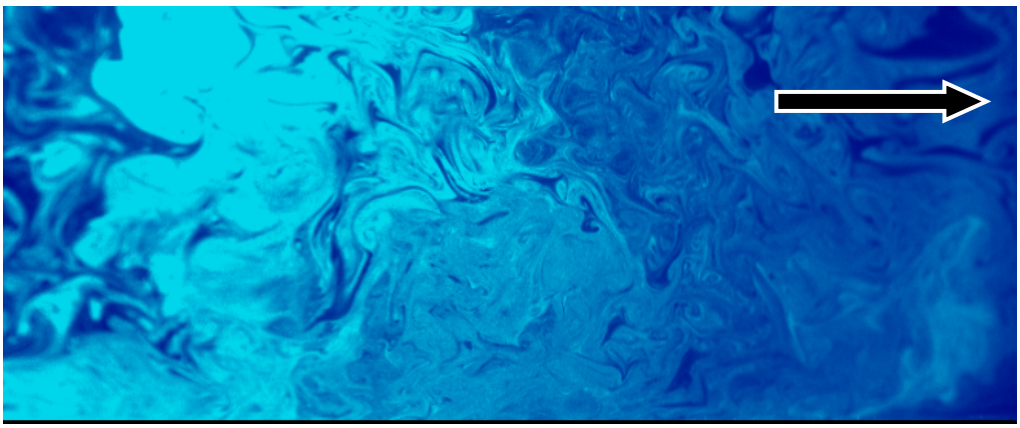

Fig. 1. Wide-range scale vortical structure of turbulent boundary layer (bottom picture side corresponds to the wall) – author's PIV visualization

2.1. Microrelief (riblets)

This technology is based mainly on the ordering of the generation of wall turbulence due to the organization of longitudinal microgrooves (so-called riblets; Fig. 2, left) that limit the intensity of pulsation motion in the transverse direction to the flow [4]. As it is known, this approach is able to provide 5-7% (and, in the most favorable conditions, over 10%) reductions in friction drag. However, its practical application faces the need for regular cleaning of microgrooves with a height of several tens of micrometers during their operation.

Nevertheless, in early 2013, Lufthansa Technik, as a result of about a year and a half of cooperation with Airbus Operations and the Fraunhofer Institute for Manufacturing Technology and Advanced Materials, announced a new paint with a structure of its external coating in the form of a shark skin relief (Fig. 2, right), which gave the technology the appropriate name "Sharkskin" and was successfully tested on two Airbus A340-300s aircrafts and provided fuel savings of 1% at a cruising speed of 810 km/h. This success inspired researchers to further improve the technology in collaboration with the world's largest German chemical concern BASF, resulting in a new adhesive film coating called AeroSHARK, which was successfully tested on a Boeing 747 for 1,500 flight hours and led to a statistically proven

similar effect of about 1% when covering 500 m^2 of the lower part of the streamlined surface area. As a result of the success achieved, it was decided to apply a new coating for all 11 Lufthansa B777 freighters and for all 12 SWISS long-haul passenger B777-300ER aircrafts starting in 2022. According to Lufthansa Technik estimates, covering 950 m^2 of the external B777 surface makes it possible to achieve annual savings of about 400 tons of kerosene and reduce harmful CO_2 emissions by more than 1,200 tons.

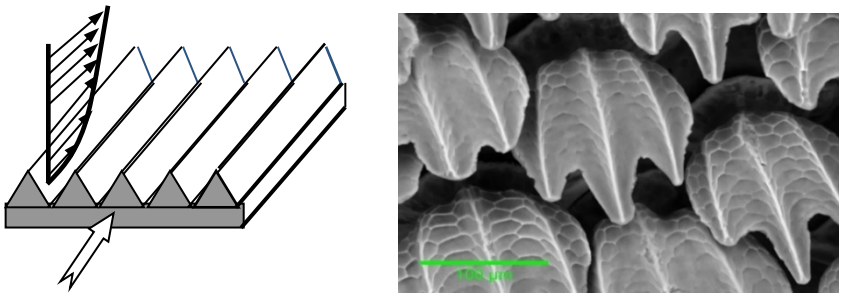

Fig. 2. Artificial microgrooves (riblets) on the streamlined surface – left, the natural microstructure (denticles) of shark skin (image from open Internet resource https://www.smithsonianmag.com/innovation/why-are-scientists-trying-to-make-fake-shark-skin-80951514/ authors: Joh. Oeffner, Li Wen, Jam. Weaver, G. Lauder) – right

Thus, this technology is mainly aimed at the dissipative vortex structure of micro-scale turbulence. As shown by its successful application by Lufthansa Technik, it is quite workable for long-haul large-sized aircraft, the cruising mode of which proceeds mainly at a considerable altitude (H=10-11 km), where the air is clean. However, in the case of high-speed trains interacting with the surface layer of air, the long-term operational applicability of such technology is questionable.

2.2. Microblowing

This technology is related to mass transfer through a streamlined surface and was developed by D. Hwang in the mid-1990s on the basis of new technologies in the production of permeable surfaces [5, 6]. The main innovation and the term microblowing imply a small air injection rate (a fraction of a percent of the main flow rate) through micro-sized holes. According to its developer, this technology is practically applicable and effective since it is able to reduce friction drag by up to 80%. However, a disadvantage is its significant need for secondary air, taking into account the wetted surface area, as well as the operational aspect of maintaining a clean, porous surface. In addition, for aircraft, this technology reduces the operational range of angles of attack due to the premature separation of the flow, which significantly limits its use, whereas, for high-speed trains, the operational problem of maintaining a clean, porous surface is the highest priority. Moreover, the cost of manufacturing large areas of permeable casing coating with high-quality micro-holes is still quite high. Nevertheless, numerical estimates [6] are very optimistic and give hope for about a 40% reduction in the aerodynamic drag of a typical Chinese high-speed train CRH380 at a microblowing speed of 0.25% of its cruising speed of 300 km/h.

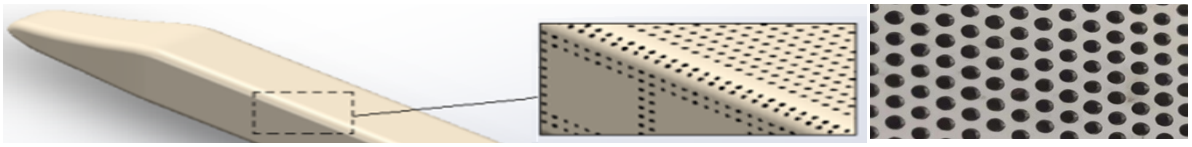

Fig. 3. The basic idea of the permeable surface of the high-speed vehicle – left, modern permeable material sample (chemical etching, ⌀0.2 mm) – right

2.3. Dimpled surface

This technology consists of creating an array of small cavities of spherical, ellipsoidal, or another similar shape (so-called dimples) on a streamlined surface (Fig. 4).

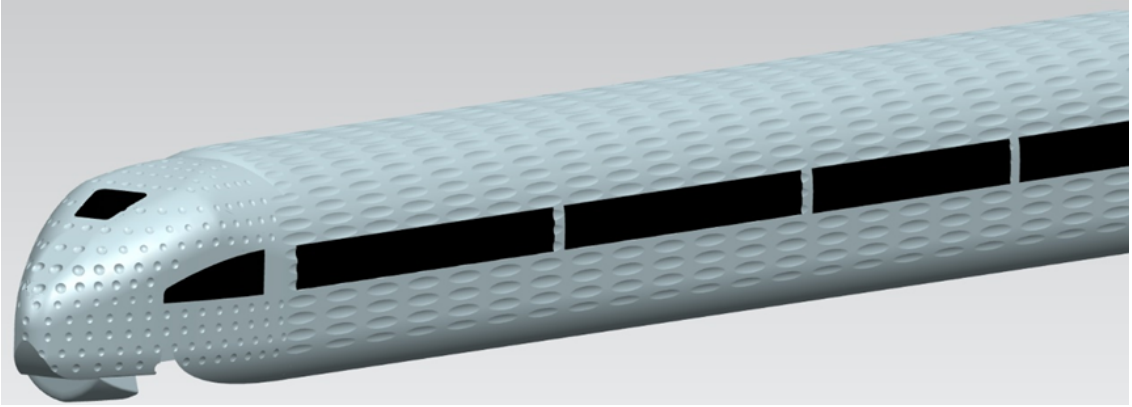

Fig. 4. The basic concept of a high-speed vehicle with a dimpled surface

It aims to create a regular near-wall vortex structure with scales commensurate with the dimensions (mainly depth) of the cavities, which redistributes turbulence energy in the longitudinal, normal, and transverse directions, suppressing the longitudinal component and intensifying the transverse one [7]. This technology has been successfully used for a long time to effectively intensify the heat exchange properties of surfaces with a concomitant slight increase in their flow resistance. However, under certain combinations of conditions, it is assumed that this approach can also reduce aerodynamic drag. The estimated positive effect is up to 17% (this is repeatedly declared as an advertisement for the technology but was unconfirmed in experiments by G. Kiknadze on a high-speed train model), but the most rational estimates do not exceed 5%. Nevertheless, research on this topic is intriguing and requires additional research since there is much contradictory information in the literature and attempts to reproduce the positive effect of some researchers in the experiments of others are often unsuccessful. Nevertheless, the ability of dimples to generate a vortex structure with the desired properties is very intriguing from the point of view of effectively controlling the properties of turbulent flow. However, a disadvantage of the technology is its rigid binding to the expected operating mode, whereas in other modes, this technology will only be a source of additional energy losses. Nevertheless, dimples, as efficient vortex generators, significantly and effectively improve the stability of the flow to separation in a wide range of operating conditions.

Thus, the main result of the small review conducted above is the potentially unexpected conclusion regarding the possible positive synergistic effect when an attempt is made to combine several of the above technologies in order to achieve a manageable persistent effect of reducing aerodynamic drag. Therefore, for further consideration, we will put forward a hypothesis about the feasibility of a combination of dimples and blowing through part of their inner surfaces. The main idea is to eliminate the need for a distributed input in such a combination and replace it with a concentrated one, and the necessary distribution of the blown jet over the area of the streamlined surface is supposed to be carried out due to the vorticity generated inside the dimples. This approach aims to reduce the total cost of the technology associated with the implementation of injection through the surface and improve its performance by eliminating finely perforated coatings.

3. DIMPLE GEOMETRY AND MODELING APPROACHES

3.1. Dimpled inserts

Based on the results of the study of dimple geometry's influence on the ability to reduce drag [8], at this initial stage, an ellipsoidal geometry of the dimples was chosen, which, according to direct numerical simulation [8], has the potential to reduce the total drag to 4.9% (unlike typical spherical dimples, which increase total drag to 6.4%). In addition, for the versatility and flexibility of both numerical and experimental testing, the 3D CAD model of a set of dimples is organized as an insert with a width of L_{ins}=35 mm and height of h_{ins}=5 mm (Fig. 5), which allows us to allocate it in different places on the test plate surface, change it to another insert with a different arrangement of dimples, and combine

several rows of inserts with similar or differently allocated dimples in different superpositions. In the present study, the distance between the leading edge of the test plate model and the line at the beginning of the dimple array was 80 mm. That is, for the entire range of free stream speeds (V_∞) studied both experimentally (up to 50 m/s) and numerically (up to 100 m/s), it can be said that the dimples are located in the laminar flow zone or, for V_∞ close to 100 m/c, in the initial zone of the transition. This is a convenient placement of the dimples in terms of assessing their turbulizing effect.

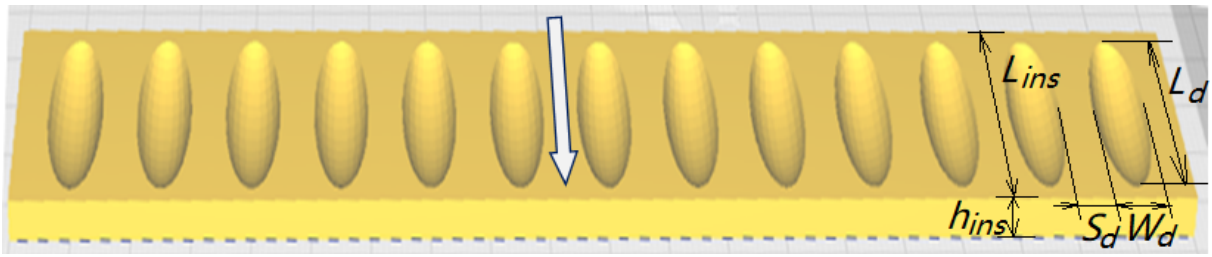

Fig. 5. A sample of an insert with a series of ellipsoidal dimples (L_d=28 mm, L_d/W_d=3.5, L_d/S_d=4.67)

3.2. Domain and computational mesh

The modeling of the effects associated with the influence of wells on wall eddy formation was simplified as much as possible by selecting a domain in the form of a rectangular parallelepiped (Fig. 6) with the following typical faces: *ABEFGHKL* – streamlined wall with dimpled insert (there can be more than one along the wall), *BCDE* – inlet, *HIJK* – outlet, *BCIH*, and *EDJK* – sides, *CDJI* – top face. In addition, the experimental and numerical research was unified through the selection of a domain length of L_{dmn}= 0.35 m and a height of H_{dmn}=0.05 m. However, the width of the region in the experiment was chosen W_{dmn}=0.2 m, whereas in numerical modeling, it was usually between two adjacent planes of symmetry in order to increase the mesh resolution and, because of symmetry, to surround one dimple or a couple of dimples. Due to the simple geometry of the domain and the shallow diploma, a structured (close to orthogonal) computational mesh with an increased resolution near the wall was generated (Fig. 7). When the mesh was constructed, the fulfillment of the traditional wall condition $y^+ = yv_*/\nu$ <1.2 was strictly controlled to provide the most important sufficient prerequisites for mesh independence, d. This led to grids from 630,000 to 2.2 million nodes, depending on the flow speed, the geometry of the simulated dimples, and the width of domain W_{dmn}, where $v_* = \sqrt{\tau_w/\nu}$, τ_w – wall shear stress in the direction of flow development, ν – kinematic viscosity coefficient.

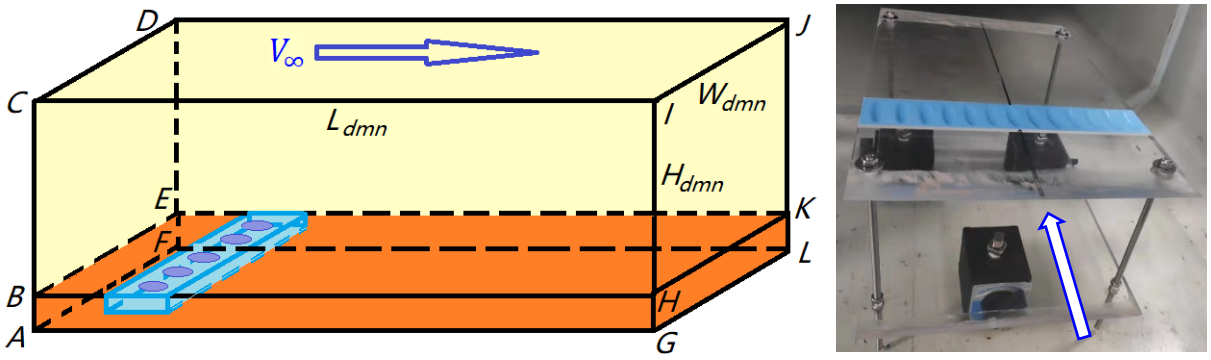

Fig. 6. The domain (left) and the corresponding experimental test rig installed in the wind tunnel (right)

3.3. Governing equations

The 3D flow around the dimpled wall was simulated by solving the following system of Reynolds-averaged Navier–Stokes (RANS) governing equations under the assumptions of stationary incompressible and predominantly turbulent airflow, completely corresponding to the formulated above operating conditions of high-speed trains with the use of the ANSYS Fluent 19.1:

$$\begin{cases} \nabla \cdot \bar{V} = 0, \\ (\overline{V} \cdot \nabla)\overline{V} = -\frac{\nabla p}{\rho} + \nabla \cdot \left(\nu \nabla \overline{V} + \overline{\sigma}_{t_{ij}}\right). \end{cases} \quad (1)$$

Here, $\bar{V}$ – flow velocity vector, p – pressure, ρ – density, and $\overline{\sigma}_{t_{ij}} = -\overline{u_i' u_j'}$ –additional Reynolds stresses resulting from the turbulent exchange dissipative mechanism. The order of accuracy of the finite-volume discretization was chosen as second, dual precision was used, and the residuals for all computational variables were taken as $\varepsilon = 1 \cdot 10^{-5}$.

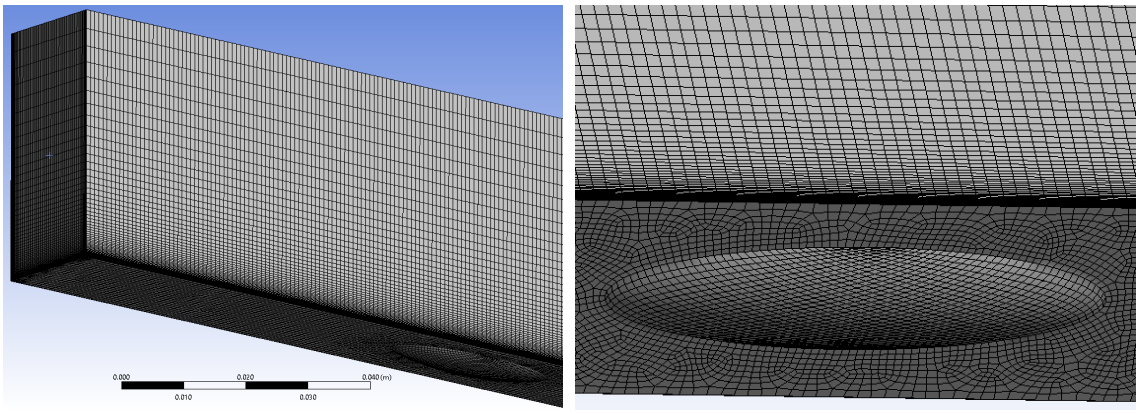

Fig. 7. Structured and close-to-orthogonal nonuniform computational mesh with increased resolution near the wall

3.4. Boundary conditions

The boundary conditions were established according to the ANSYS Fluent formalism as follows: streamlined surface *ABEFGHKL* (wall) – velocity magnitude 0 m/s (no-slip); inlet face *BCDE* – velocity magnitude $V_x = V_\infty =$ 5-100 m/s (excluding the top wall face with dimple surface *BEFG*, where $V_x = 0$ m/s); lateral faces *BCIH*, *EDJK* – symmetry; outlet face *HIJK* – gauge pressure 0 Pa (pressure-outlet).

3.5. Turbulence model

According to the Boussinesq approach, Reynolds stresses can be directly connected with the strain rate tensor components similarly to the laminar case but by the use of additional viscosity (so-called eddy- or turbulent viscosity ν_t), which reflects the dissipative mechanism of the turbulence:

$$\overline{\sigma}_{tij} = -\overline{u_i' u_j'} = \nu_t \overline{S}_{ij}, \nu_t = \mu_t / \rho. \quad (2)$$

On the basis of the RANS approach, the turbulent viscosity ν_t must be modeled with the use of an additional semi-empirical model of turbulence. Within the framework of ANSYS software, it is impossible to completely take into account the influence of blowing on the level of any of the turbulence models available therein, and this is the reason for adding some computational code. As follows from the obtained results, the two-equation low-Reynolds version of the *k-ω* Shear Stress Transport (SST) turbulence model with a curvature correction allows us to get realistic results, and it is well adjusted to the wall vicinity region. Moreover, due to the low-Reynolds adaptation, this model is able to approximately reproduce the process of laminar-turbulent transition in the boundary layer. Due to these reasons, the *k-ω* SST turbulence model was used as the basis of further computations.

3.6. Mass exchange through the streamlined surface

The mass transfer factor through the streamlined surface was taken into account through modifications of fluxes of mass, momentum, and the turbulence model parameters through the wall faces of mesh cells in local areas where wall permeability is assumed by using specially developed user-defined functions that determine the permeable sections geometry and mass-exchange direction and rate

through the streamlined surface. The obtained numerical solutions were additionally tested to implement the integral mass balance at the outer boundary of the computational domain and the streamlined surface.

3.7. Experimental equipment and measurements

We used the experimental setup shown in Fig. 6 (right) in a certified wind tunnel at the College of Engineering at the Zhejiang Normal University, which has two octagonal test sections: a large low-speed flow area (1,050*1,050*1,500 mm) with a speed of up to 20 m/s and a small high-speed flow area (600*600*1500 mm) with a speed up to 60 m/s. The flow speed's spatial, angular, and temporal inhomogeneities do not exceed 0.16%, 0.8º, or 0.05%, respectively, and the turbulence intensity level is $Tu \leq 0.5\%$. The measurements were carried out using the 3D time-resolved particle image velocimetry system, developed by LaVision Co. and based on: a dual cavity high-speed Nd:YAG laser with repetition rate 0.2-10 kHz and output energy of 30 mJ (x2) at 527 nm @ 1 kHz; two cameras (FASTCAM Mini AX200) with a CMOS sensor resolution of 1024 x 1024 pixels, a frame rate of 6400 fps (PIV data sample frequency 3,200 Hz), a pixel size of 20 μm x 20 μm, memory of 16 GB, sensitivity ISO 40000 mono, ISO 16000 color, lens Tokina 100 mm AT-X Pro Macro 100 F2.8 D, a focal length of 70-300 mm (zoom), aperture of f/2.8-f/16; an aerosol generator that uses dioctyl sebacate liquid for particle generation with average diameter 19 μm, and LaVision Davis 10.2.1 software (Fig. 8).

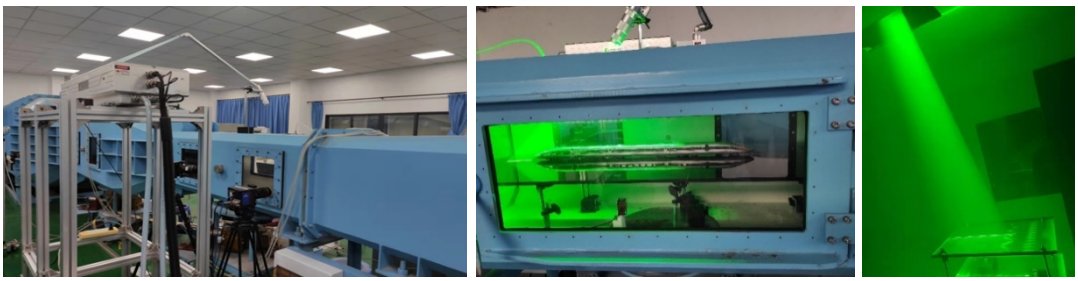

Fig. 8. Experimental equipment of the wind tunnel laboratory of the College of Engineering at the Zhejiang Normal University (Jinhua, China)

4. RESULTS AND DISCUSSION

4.1. Flow over ellipsoidal dimples

The large-scale computational and physical experiment (based on both RANS in a wide range of speeds with differently oriented dimples of different geometries and locations) allowed us to confirm the following well-known facts:

1. Dimples are very effective wall localized vortex generators localized on a streamlined surface. Moreover, although PIV measurement technology has a relatively low accuracy near streamlined surfaces due to interference caused by unavoidable and completely irreversible reflections of the laser beam, measurements show an increase and intensive propagation of disturbances in the boundary layer directly behind the array of dimples (Fig. 9).
2. The vortex generation effect is initiated mainly on the front half of the concave surface of the dimple (looking in the flow development direction) due to a locally formed diffusor channel (a zone of an adverse pressure gradient), which, already at the relative depth of the ellipsoidal dimple $h_d/L_d \approx 0.035$, contributes to a nonuniform pre-separate and, at greater depths, to the separation state of the boundary layer (Fig. 10a).
3. The process of forming a vortex system in the dimple ends at the second narrowing half of its longitudinal length L_d, where the boundary layer is reattached and its inhomogeneous acceleration occurs, which leads to intensive turbulence generation in this local zone (Fig. 10b).

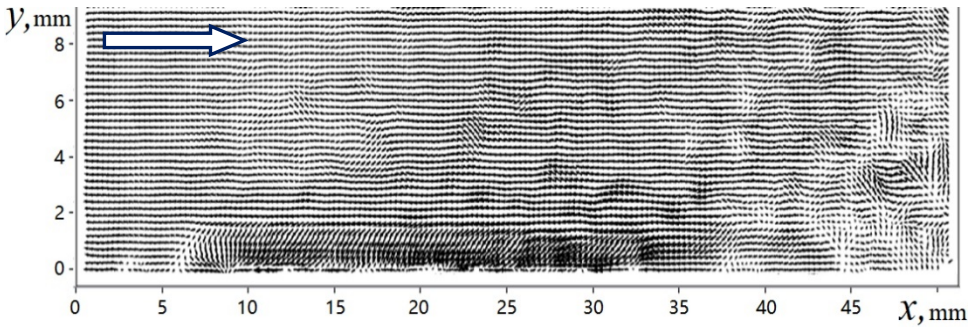

Fig. 9. Experimental PIV distribution of the instantaneous velocity in the vicinity and behind the dimple with depth of h_d=3 mm in its midplane. The ellipsoidal dimple is located between x=5 mm and x=33 mm, V_∞ =10 m/s

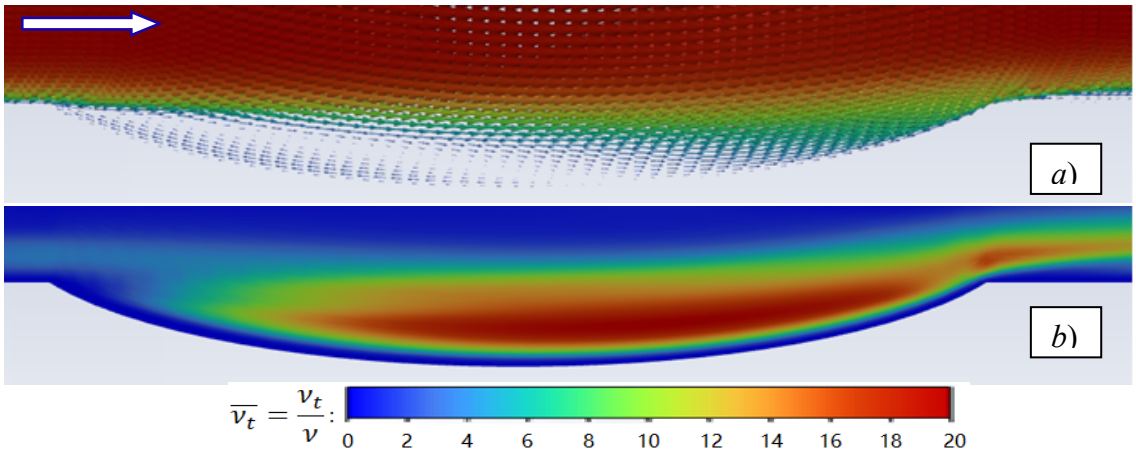

Fig. 10. Numerical RANS-based distribution of the mean velocity (*a*) and turbulence viscosity ratio $\overline{\nu_t} = \nu_t/\nu$ (*b*) in the vicinity of the dimple with a depth of h_d=3 mm in its *Oxy* midplane, V_∞ =10 m/s

4. Thus, only very shallow dimples can be used to reduce the total drag.
5. Any processes of additional large-scale vortex formation, as well as the process of increasing wall turbulence, require additional flow energy consumption. In confirmation of this physically obvious fact, we, as well as numerous researchers of dimpled surfaces [9, 10], in a wide range of conditions and geometric dimensions of dimples, failed to reproduce the effect of reducing the impedance; on the contrary, its growth was 1-7% depending on the simulated conditions.
6. Thus, the dimples themselves, even with confirmation of their ability to reduce total aerodynamic drag under certain conditions, remain a very unreliable technology for its practical implementation. However, the ability of dimples to generate a vortex structure near the surface can be used very effectively when combining dimples with blowing through the locally permeable surface, which is presented and analyzed in more detail in the next section.

4.2. Flow over ellipsoidal dimples with locally organized blowing

In this part of the study, we have considered a combination of a dimple and a uniform air jet injection inside it as an alternative to distributed microblowing through a finely perforated surface for two different locations of air injection – front (case 1) and rear (case 2) (Fig. 11).

First of all, it was established that the rear location of the injection area (case 2) is significantly more efficient than the front one (efficiency increased by up to 20-30%) due to the displacement of the flow from the wall in the narrowing part of the dimple (the zone of a favorable pressure gradient; Fig. 12a). Contrarily, the placement of the injection area in the front dimple part leads only to an intensification of the unfavorable flow separation under conditions of local diffuse flow, which leads exclusively to additional losses of flow energy and contributes to an additional increase of its turbulence. It is important to note that the last factor of turbulence intensification in the dimple is inevitable at any location of the injection area, and in the case of a rear injection location, it also increases to 25% in relation to the case

of the absence of injection. However, the effect of pushing the average flow in the area of injection leads to a decrease in the drag of the flow around the dimple (Fig. 12b).

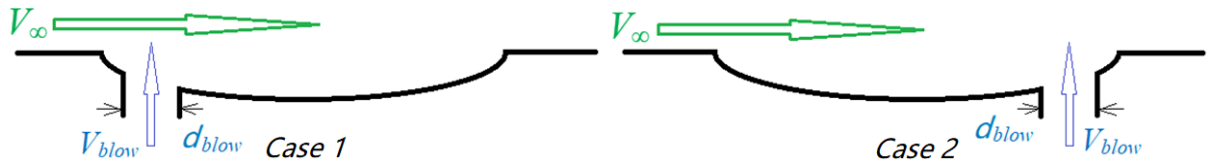

Fig. 11. Design of a combination of a dimple and uniform air jet injection

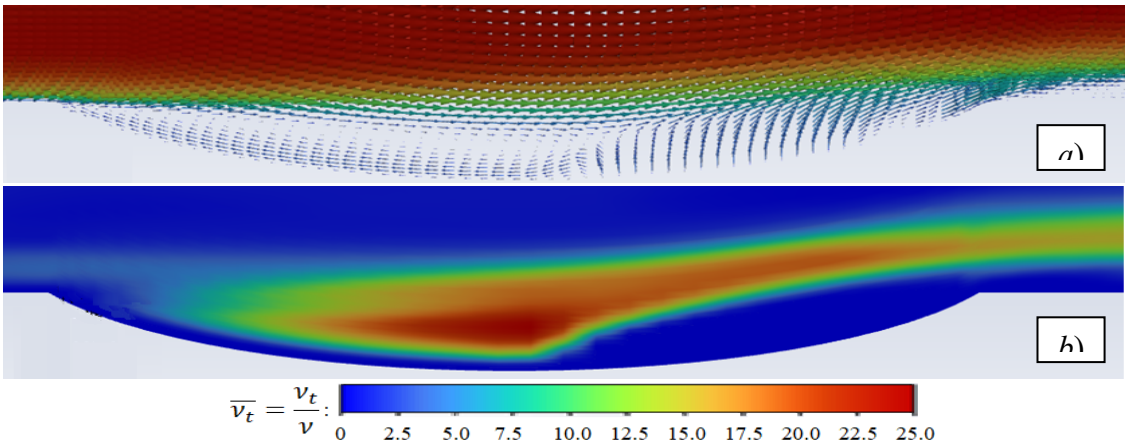

Fig. 12. Numerical RANS-based distribution of the mean velocity (*a*) and $\overline{\nu_t} = \nu_t/\nu$ (*b*) in the vicinity of the dimple with rear blowing in *Oxy* midplane (h_d=3 mm, V_∞ =10 m/s, V_{blow} =0.15 m/s)

5. CONCLUSIONS

1. The analysis of priority directions of aerodynamic improvements to the surface of high-speed vehicles is carried out and justifies the priority and potential of the methodology for improving the structure of the streamlined surface in comparison with the optimization of the shape.
2. It has been established that dimples are not a practically promising technology for drag reduction. However, in combination with locally organized blowing, their ability to effectively generate near-wall vorticity can significantly reduce the requirements for a finely permeable surface and reliably distribute locally blown air over a streamlined surface.
3. With the diameter of the air supply channel to the dimple of 10 mm and a local blowing velocity of 1.5% of the external flow speed, due to the use of such a combined technology, the estimated reduction in total drag for every square meter of the streamlined surface area was 10-12%.
4. Further developments of the proposed technology will focus on improving the combination of geometry parameters of dimples and their allocation with geometric and kinematic characteristics of blowing, as well as their adjustment to the external boundary layer parameters in order to reduce both total drag and additional fluid consumption.

Acknowledgment

This research was supported by the Ministry of Science and Technology of PR China within the framework of the Intergovernmental Chinese-Ukrainian project of scientific-technological cooperation and exchanges for 2022-2023 (the grant N KYZ04Y22152).

References

1. Schrauf, G. Status and perspectives of laminar flow. *The Aeronautical Journal.* 2005. Vol. 109(1102). P. 639-644. DOI: 10.1017/S000192400000097X.

2. Orellano, A. & Sperling, S. Aerodynamic improvements and associated energy demand reduction of trains. In: Browand, F. & McCallen, R. (eds.) *The Aerodynamics of Heavy Vehicles II Trucks, Buses and Trains.* Springer. 2009. P. 219-231. DOI: 10.1007/978-3-540-85070-0_19.
3. Corke, T.C. & Guezennec, Y.G. & Nagib, H.M. *Modification in Drag of Turbulent Boundary Layers Resulting from Manipulation of Large-Scale Structures*. NASA CR-3444. 1981. 28 p.
4. Bechert, D.W. & Bruse, M. & Hage, W. & Van der Hoeven, J.G.T. & Hoppe, G. Experiments on drag-reducing surfaces and their optimization with an adjustable geometry. *J. Fluid Mech.* 1997. Vol. 338. P. 59-87. DOI: 10.1017/S0022112096004673.
5. Hwang, D.P. *A Proof of Concept Experiment for Reducing Skin Friction by Using a Micro-Blowing Technique.* NASA TM 107315. 1996. 13 p. DOI: 10.2514/6.1997-546.
6. Shkvar, Ye.O. & Jamea, A. & Shi-Ju, E. & Cai, J.-Ch. & Kryzhanovskyi, A.S. Effectiveness of blowing for improving the high-speed trains aerodynamics. *Thermophysics & Aeromechannics. ITTF SB RAS.* 2018. Vol. 25(5). P. 675-687. DOI: 10.1134/S0869864318050049.
7. Van Nesselrooij, M. & Veldhuis, L.L.M. & Van Oudheusden, B.W. & Schrijer, F.F.J. Drag reduction by means of dimpled surfaces in turbulent boundary layers. *Experiments in Fluids.* 2016. Vol. 57. P. 142. DOI: 10.1007/s00348-016-2230-9.
8. Ng, J.H. & Jaiman, R.K. & Lim, T.T. & Tay, C.M. & Khoo, B.C. Geometric Effects of Shallow Dimples in Turbulent Channel Flows at Re≈180: A Vorticity Transport Perspective. *Flow, Turbulence and Combustion.* 2020. 40 p. DOI: 10.1007/s10494-020-00112-6.
9. Spalart, P.R. & Shur, M. & Strelets, M. & Travin, A. & Paschal, K.B. & Wilkinson, S.P. Experimental and numerical study of the turbulent boundary layer over shallow dimples. *International Journal of Heat and Fluid Flow*. 2019. Vol. 78. No. 108438. DOI: 10.1016/j.ijheatfluidflow.2019.108438.
10. Lienhart, H. & Breuer, M. & Koksoy, C. Drag reduction by dimples? – A complementary experimental/numerical investigation. *International Journal of Heat and Fluid Flow*. 2008. Vol. 29. P. 783-791. DOI: 10.1016/j.ijheatfluidflow.2008.02.001.

Received 07.12.2022; accepted in revised form 06.03.2024